frontiers in Physics

ORIGINAL RESEARCH
published: 22 July 2021
doi: 10.3389/fphy.2021.732236

Cost-Efficient Hybrid WDM-MDM-Ro-FSO System for Broadband Services in Hospitals

Peidong Liang[1], *Chentao Zhang*[1,2]*, *Jamel Nebhen*[3], *Sushank Chaudhary*[4] *and Xuan Tang*[4]

[1]Fujian (Quanzhou) – HIT Research Institute of Engineering and Technology, Quanzhou, China, [2]Department of Instrumental and Electrical Engineering, Xiamen University, Xiamen, China, [3]Prince Sattam bin Abdulaziz University, College of Computer Science and Engineering, Alkharj, Saudi Arabia, [4]Quanzhou Institute of Equipment Manufacturing, Haixi Institutes, Chinese Academy of Sciences, Jinjiang, China

The expansion of high-speed communication needs due to explosive growth of subscribers each year has led the researchers to design the next generation communication systems which can cope with the current growing demand. Millimeter waves, operated within the range of 30 GHz to 300 GHz, can become potential carrier for delivering large amount of data. However, in hospital scenarios, these radio waves are subjected to strict regulations due to direct impact on patients' health as well as high interference with other medical devices which again imposes critical challenge on patients. Thus, it is a challenge for the researchers to provide communication/broadband services for transmission of such sensitive biomedical sensor data in hospitals locations. Radio over Free space (Ro-FSO) systems may become the attractive solution to deliver millimeter waves over free space link with high speed. Further, to expand the capacity of Ro-FSO systems, mode division multiplexing (MDM) plays a vital role in addition to wavelength division multiplexing (WDM) scheme. In this work, we have demonstrated the MDM-WDM scheme to deliver four channels with each one having the capacity of 10 Gbps up-converted to 40 GHz over FSO link which is suitable for providing broadband and communication services within the hospital premises. Moreover, the proposed WDM-MDM-Ro-FSO link is evaluated under different fog conditions.

Keywords: broadband services, radio over free space optics, mode division multiplexing, hospital scenarios, health monitoring

OPEN ACCESS

Edited by:
Santosh Kumar,
Liaocheng University, China

Reviewed by:
Akhilesh Pathak,
Chulalongkorn University, Thailand
Sudhanshu Arya,
Pukyong National University, South Korea

***Correspondence:**
Chentao Zhang
zctyyy@163.com

Specialty section:
This article was submitted to Optics and Photonics, a section of the journal Frontiers in Physics

Received: *28 June 2021*
Accepted: *07 July 2021*
Published: *22 July 2021*

Citation:
Liang P, Zhang C, Nebhen J, Chaudhary S and Tang X (2021) Cost-Efficient Hybrid WDM-MDM-Ro-FSO System for Broadband Services in Hospitals. Front. Phys. 9:732236. doi: 10.3389/fphy.2021.732236

INTRODUCTION

The demand of wireless communication has increased rapidly since last decade which led to the development of optical wireless communication systems. International Telecom Union (ITU) [1] reported that the total number of mobile broadband subscribers increases every year by 20% that crossed four billion by the end of 2017. This growth further levitates the challenges for ITU to assign radio frequency (RF) spectrum for different cellular operators, both in rural and urban areas. However, in hospital scenarios it is not always feasible to provide broadband services due to interference of radio signals with sensitive medical appliances as well as having high impact on patients' health [2]. Thus, the use of radio waves is prohibited in hospital locations. However, broadband services are necessary in hospitals to transmit valuable data such as patients' monitoring reports from one location to another. Not only this, with high-speed broadband services doctors can connect with one another at any time and access the medical data bases from any location. This

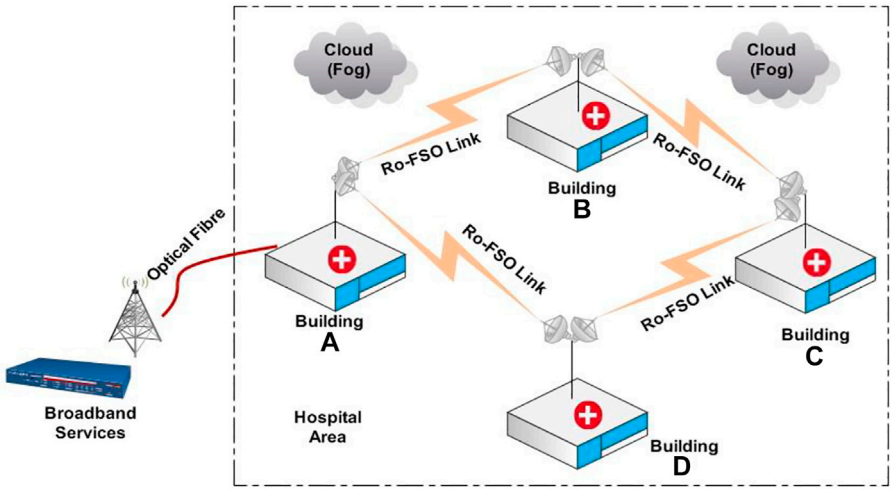

FIGURE 1 | Ro-FSO system in Hospital Infrastructure.

potential usage of broadband services further posits a big challenge for broadband providers to provide in the hospitals without compromising the health of patients. Ro-FSO or radio over free space can provide broadband services in hospitals as it integrates radio and optical networks as shown in **Figure 1**.

Ro-FSO permits the multiple transmission of RF signals without any expensive optical fiber infrastructure as well as license to RF operators [3]. Also, as data transmission in Ro-FSO is in the form of light signals which has no impact on patients' health as well as no interference with the medical devices, it becomes an attractive solution for providing broadband services in hospitals. Moreover, in hospital areas, it is not feasible to dig for installing optical fiber cables due to need of continuous working operations and less space, thus Ro-FSO becoming an apt substitute for replacing the optical fiber infrastructures. It also combines RoF or radio over fiber and FSO or free space optics. RoF allows sharing of various expensive RF operations like up-conversion and down-conversion, handoff, switching, etc. from central location to all the base stations which results in reduction of deployment cost [4]. Moreover, it can share large-bandwidth RF signals with low attenuation and power consumption. Whereas, FSO does not use optical fibers. Instead, it enables atmospheric data transmission with rapid adoption [5, 6]. Also, in contrast to RF transmission, it does not need any license. These combined features of RoF and FSO make Ro-FSO a compatible technology for providing broadband services in hospitals. Therefore, Ro-FSO is a relevant technology for seamless, rapid and cost-effective integration with RF wireless networks [7, 8]. However, Ro-FSO faces challenges of atmospheric turbulences such as scintillations, fog, rain, snow, etc. affecting the signal to noise ratio [9]. These atmospheric turbulences increase attenuation in the transmission path which results in shutdown of the network. Thus, researchers should consider these turbulences while designing the Ro-FSO network. Another emerging technology is MDM or mode division multiplexing that transmits through multiple channels using different modes. Apart from wavelength [10], polarization [11] and time [12] multiplexing schemes, MDM enables multimode data transmission by multiplexing through a single optical channel. In MDM, modes can be excited through various mechanisms such as spatial light modulators [13], offset launch [14], high-speed VCSEL arrays [15] and photonic crystal fibers (PCF) [16]. Researchers have used four OAM beams (1 = ±1 and 1 = ±3) to transmit 400 Gbps data through an FSO link of 120 m in 2016 [17]; MDM-OFDM scheme to transmit 80 Gbps data through an FSO link of 50 km in 2017 [7]; and MDM-based polarisation phase shift key scheme to transmit 80 Gbps data through an FSO link of 90 km in 2020 [18]. Researchers have also proposed hybrid multiplexing-based multi-channel communication systems including wavelength division multiplexing (WDM)-MDM [19], Optical code division multiplexing (OCDMA)-MDM [20] and WDM-PDM [21]. Combining MDM with WDM can increase aggregate capacity and improve spectral efficiency of Ro-FSO infrastructures which has potential application in hospital infrastructures. In this work, we have demonstrated Ro-FSO topology specially designed for medical locations by incorporating the WDM-MDM scheme which can transmit four channels with the each one having capacity of 10 Gbps up-converted to 40 GHz radio signal each over FSO link.

MDM-RO-FSO MODELING

The schematic diagram of the proposed MDM-Ro-FSO is shown in **Figure 2**. Four channels are transmitted by using the hybrid WDM-MDM scheme. For the WDM scheme, two wavelengths (850 nm and 851 nm), each with 1 nm channel space, are used. The MDM scheme uses modal multiplexing of LG (Laguerre Gaussian) 00 and HG (Hermite Gaussian) 00. As shown in **Figure 2**, first and second channels are operated on LG 00 and HG 00 modes respectively with the wavelength of 850 nm while third and fourth channels are operated on LG 00 and HG 00 modes respectively with the wavelength of 851 nm. LG and HG modes are described by following **Eq. 1** and **Eq. 2** [22]:

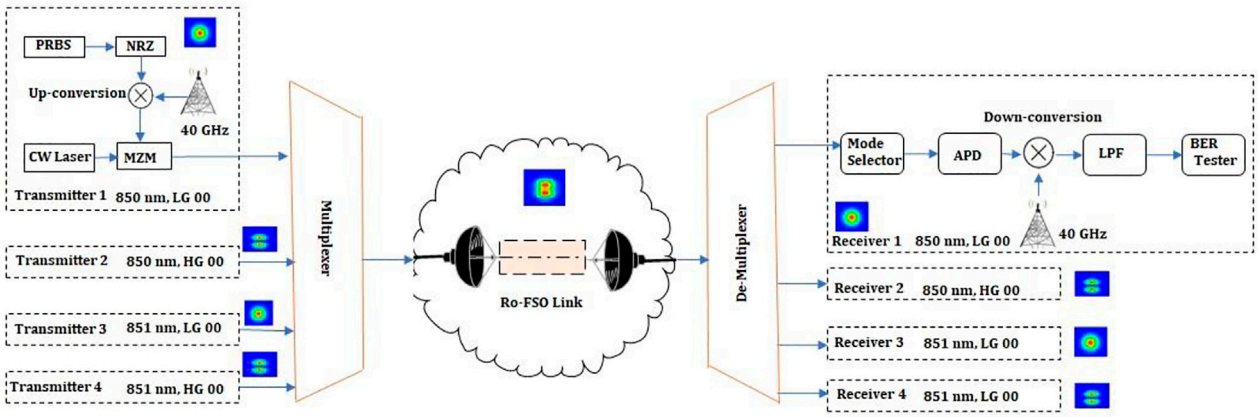

FIGURE 2 | Proposed 4 x 10 Gbps Ro-FSO Link.

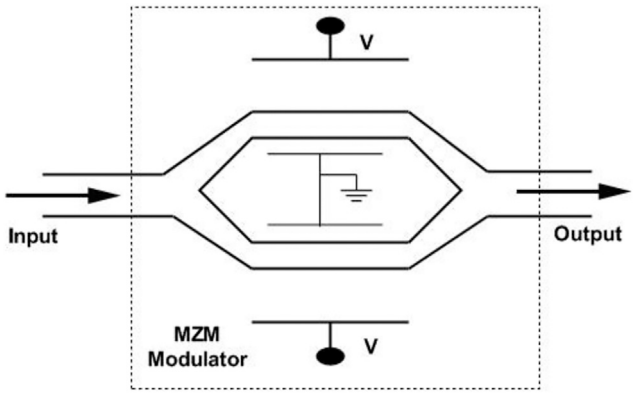

FIGURE 3 | Schematic model of MZM modulator.

$$\psi_{m,n}(r,\varphi) = \left(\frac{2r^2}{\omega_o^2}\right)^{\left|\frac{n}{m}\right|} L_m^n\left(\frac{2r^2}{\omega_o^2}\right)\exp\left(\frac{r^2}{\omega_o^2}\right)\times \exp\left(j\frac{\pi r^2}{\lambda R_0}\right)\left\{\begin{array}{l}\sin(|n|\varphi), n\geq 0\\ \cos(|n|\varphi), n\geq 0\end{array}\right\} \quad (1)$$

The above equation contains the azimuthal index *(X)* represented by *m* and the radial index (*Y)* represented by *n*. Curvature radius is represented by R_o, spot size by w_o and the Laguerre Polynomial by *Ln, m*.

$$\psi_{m,n}(r,\phi) = H_m\left(\frac{\sqrt{2}x}{w_{o,x}}\right)\exp\left(-\frac{x^2}{w_{o\,x}^2}\right)exp\left(j\frac{\pi x^2}{\lambda R_{o\,x}}\right)\times H_n\left(\frac{\sqrt{2}y}{w_{o,y}}\right)\exp\left(-\frac{y^2}{w_{o\,y}^2}\right)\left(j\frac{\pi y^2}{\lambda R_{o\,y}}\right) \quad (2)$$

In the above equation, the X and Y indexes represent mode dependencies on their axes denoted by *m* and *n*, respectively. The radius of curvature is denoted by R_o and *wo* is the spot size. Hermite polynomials are denoted by Hm and *Hn*.

Each channel has a non-return to zero (NRZ) data of 10 Gbps mixed with 40 GHz mm wave generated by sine generator with the help of mixer for the process of up-conversion. This 40 GHz mm wave is modulated over optical carrier by using Machzehnder modulator (MZM) derived from spatial continuous wavelength laser. The schematic diagram of MZM modulator is shown in **Figure 3**. The working principle *of MZM modulator*of MZM modulator is given by the following equation [23]:

$$E_{out}(t) = E_{in}(t).\cos(\Delta\theta(t)\times\exp(j.\Delta\Phi(t)) \quad (3)$$

where E_{out} (t) is the electrical field at output port of modulator, E_{in} (t) is the electrical field at input port of modulator, phase difference between two branches are represented by$\Delta\theta(t)$ which can be further represented as:

$$\Delta\theta(t) = \frac{\Pi}{2}\times(0.5 - ER\times(Modulation(t) - 0.5)) \quad (4)$$

where *Modulation (t)* is the electrical input signal.

In the above equation, the term *ER* can be defined as:

$$ER = 1 - \frac{4}{\Pi}\times\arctan\left(\frac{1}{\sqrt{extract}}\right) \quad (5)$$

where *extract* is the extinction factor which is set to be 30 dB. Similarly, signal phase change is defined as:

$$\Delta\Phi(t) = SC\times\Delta\theta(t)\times\frac{1+SF}{1-SF} \quad (6)$$

where the value of *SC* is 1 if the negative chirp value is enabled; otherwise, it will be -1 and *SF* is the symmetry factor.

The output of optical modulator is combined with the output of three modulators from different channels and transmitted over FSO link followed by optical amplifier with a gain of 16 dB. The link can be defined by the following equation [24]:

$$P_{Received} = P_{Transmitted}\frac{d_R^2}{(d_T+\theta_R)^2}10^{\alpha R/10} \quad (7)$$

TABLE 1 | Key parameters.

Item	Parameter	Value
PRBS	Data rate	10 Gbps
Sine generator	RF carrier	40 GHz
Spatial laser	Wavelength	850 and 851 nm
	Power	0 dBm
	Linewidth	10 MHz
Machzhender modulator	Extinction ratio	30 dB
	Symmetry factor	1
FSO link	Transmitter aperture diameter	10 cm
	Receiver aperture diameter	20 cm
	Beam divergence	2 μrad
Spatial APD photo diode	Width	10 µm
	Responsivity	1.2 A/W
	Gain	3
	Dark current	10 nA
	Responsivity	1 A/W
	Thermal noise power spectral density	100e-024 W/Hz
	Ionization ratio	0.9

The equation above represents receiver aperture diameter (d_R), transmitter aperture diameter (d_T), beam divergence (θ), range (R) and atmospheric attenuation (α). Gamma distribution model is used to model the atmospheric fading. The probability of given intensity (I) is described in the following equation [25]:

$$P(I) = \frac{2(\alpha.\beta)^{(\alpha+\beta)/2}}{\Gamma(\alpha)\Gamma(\beta)} I^{\left(\frac{(\alpha+\beta)}{2}\right)-1} K_{\alpha-\beta}\left(2\sqrt{\alpha.\beta.I}\right) \quad (8)$$

In the above equation, small-scale eddies are represented by$1/\alpha$, large-scale eddies are represented by $1/\beta$, $\Gamma(\ldots)$is the Gamma function and $K_{\alpha-\beta}$is the modified Bessel function of second kind. α and β can be derived mathematically as shown in **Eq. 9** and **Eq. 10**:

$$\alpha = \exp\left[\frac{0.49\sigma_R^2}{\left(1+1.11\sigma_R^{12/5}\right)^{5/6}}\right] - 1 \quad (9)$$

$$\beta = \exp\left[\frac{0.51\sigma_R^2}{\left(1+0.69\sigma_R^{12/5}\right)^{5/6}}\right] - 1 \quad (10)$$

where σ_R^2 is the Rytov variance which can be calculated from the following equation:

$$\sigma_R^2 = 1.23 C_n^2 k^{7/6} z^{11/6} \quad (11)$$

where C_n^2 is the index refraction structure, k is the optical wavenumber and z is the range.

Atmospheric attenuation for FSO link is considered as 0.14 dB/km in clear weather, 12 dB/km in low fog, 16 dB/km in medium fog and 22 dB/km in heavy fog [26, 27]. A splitter is used to split the FSO output

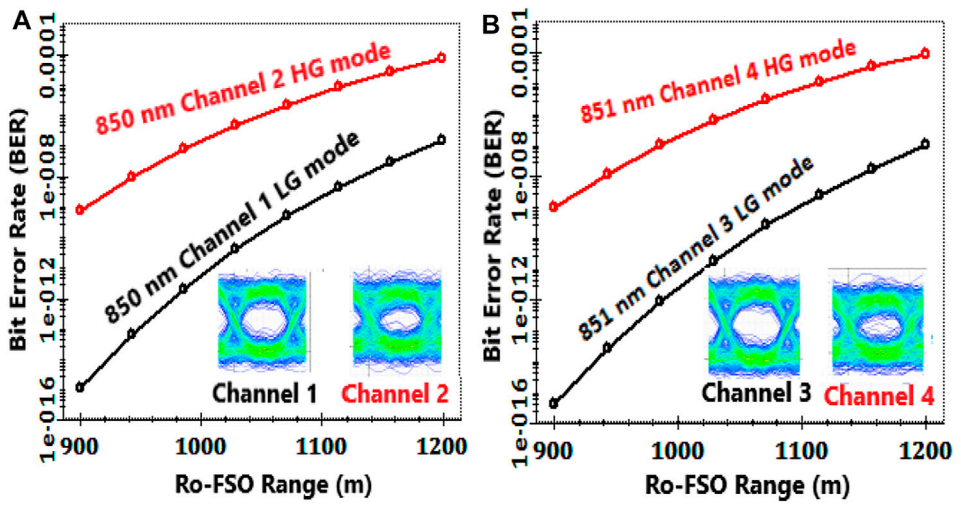

FIGURE 4 | Measurement of BER **(A)** Channels 1 and 2 **(B)** Channels 3 and 4.

into four receivers. Each receiver consists of a mode selector which selects the particular mode and wavelength. APD or avalanche photo diode is used for converting the optical signal to an electrical signal.

The shot noise and thermal noise is enabled in the APD whereas other background noises are assumed to be ideal in this work. After 40 GHz is mixed for the down-conversion process, the original baseband signal is recovered by using low pass filter.

The other key parameters are mentioned in **Table 1**.

RESULTS AND DISCUSSION

The modeling of the proposed MDM-Ro-FSO model is done in OptiSystem™ software due to its accuracy. In this section, results obtained from the modeling are presented and discussed. First, Ro-FSO link is operated in clear weather conditions which mean no atmospheric turbulences are considered. The BER or bit error rate for all channels is measured as shown in **Figure 4**. At the distance of 1,200 m, the BER value for Channel 1 transmitted by using LG mode at 850 nm wavelength is computed as 10^{-7} whereas for Channel 2, which is transmitted by using HG 00 mode, it is computed as 10^{-5}.

The result shows that HG mode is slightly more attenuated in FSO link as compared to LG mode. Similarly, the value of BER for Channel 3 transmitted by using LG 00 mode with 851 nm is also computed as 10^{-7} whereas for Channel 4, which is transmitted by using HG 00 mode, it is computed as 10^{-5}. This shows that all the

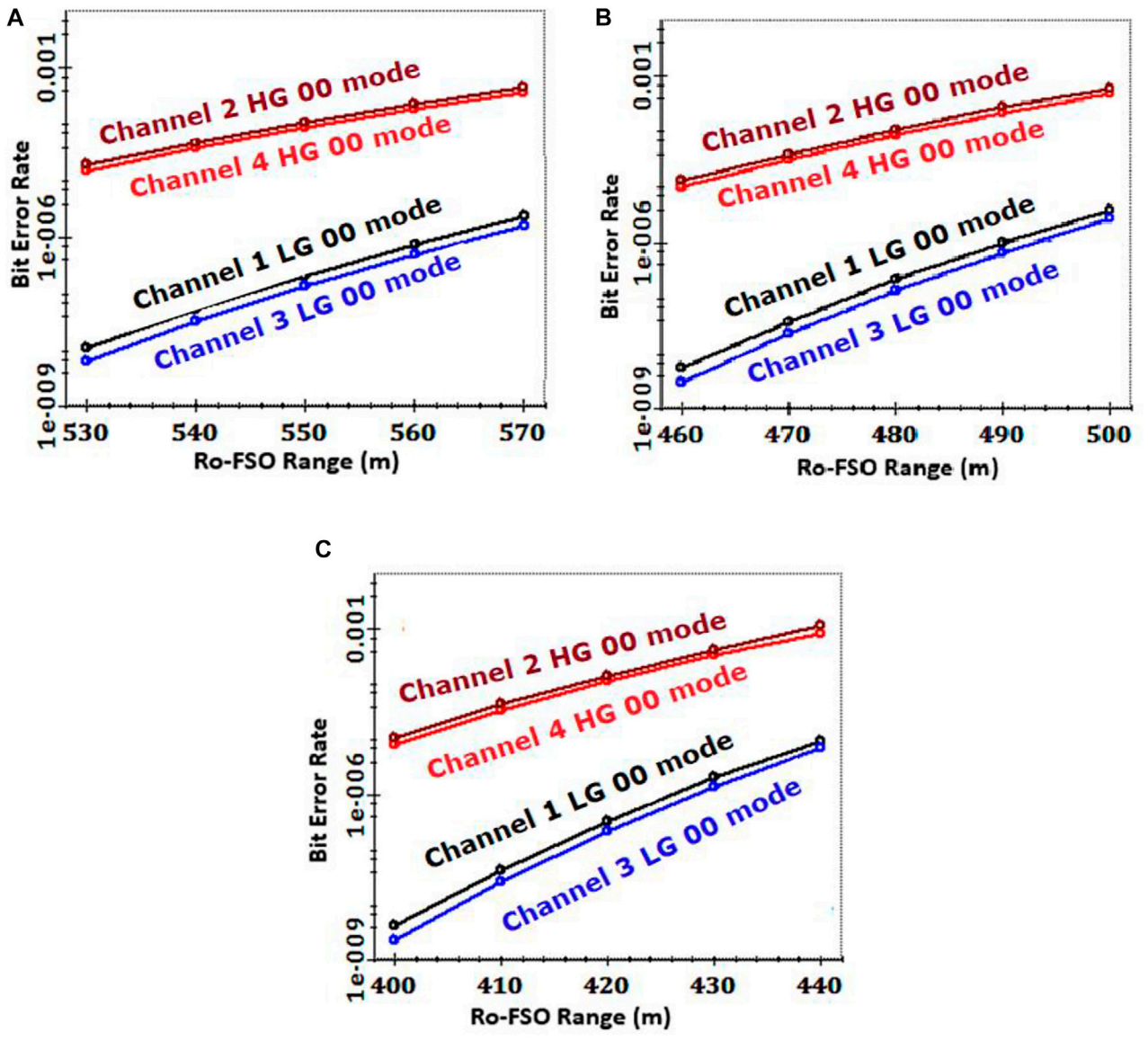

FIGURE 5 | Measurement of BER **(A)** low fog **(B)** medium fog **(C)** heavy fog.

channels are transmitted successfully over 1,200 m Ro-FSO link with acceptable BER ($\leq 10^{-3}$).

After that, the proposed MDM-Ro-FSO link is operated under the influence of different fog conditions that is low, medium and high. For low fog conditions, the value of atmospheric attenuation is considered as 12 dB/km whereas for medium fog conditions it is considered as 16 dB/km and for heavy fog conditions, it is considered as 22 dB/km. **Figure 5** (a), (b) and (c) show the measurement of BER of all channels under low, medium and heavy fog. When the Ro-FSO link is operated under low fog, the BER value for channel 1 and 3 is computed as 10^{-6} whereas for channel 2 and 4, it is measured as 10^{-4} at the Ro-FSO link distance of 570 m. However, when the Ro-FSO link is operated under medium fog, the BER value for channel 1 and 3 is computed as 10^{-5} whereas for channel 2 and 4, it is measured as 10^{-3} at the Ro-FSO link distance of 500 m. Similarly, when the Ro-FSO link is operated under heavy fog, the BER value for channel 1 and 3 is measured as 10^{-5} whereas for channel 2 and 4, it is measured as 10^{-3} at the Ro-FSO link distance of 440 m only.

CONCLUSION

In this work, low-cost high-speed Ro-FSO system is proposed for providing broadband services in hospital scenarios. WDM and MDM schemes are incorporated to transmit four channels with the capacity of 10 Gbps each up-converted to 40 GHz mm wave over Ro-FSO link. The MDM scheme uses LG 00 and HG 00 modes whereas WDM uses 850 and 851 nm wavelengths. The reported results indicate successful transmission of all channels. When the RO-FSO link is operated in clear weather, all the channels are successfully transmitted up to 1,200 m. However, when the Ro-FSO link is operated in low, medium and heavy fog, the transmission distance is limited to 570, 500 and 440 m, respectively with acceptable ($\leq 10^{-3}$). Further research of the current work can include real-time experiments and performance evaluation of MDM-Ro-FSO under different atmospheric conditions.

DATA AVAILABILITY STATEMENT

The raw data supporting the conclusions of this article will be made available by the authors, without undue reservation.

AUTHOR CONTRIBUTIONS

PL: Conceptualization, methodology, investigation, writing—original draft, supervision, resources, project administration, funding acquisition. CZ: Methodology, investigation, writing—original draft, supervision, funding acquisition. JN: Methodology, investigation, data curation, visualization. SC: Investigation, data curation, writing—original draft. XT: Writing—review andediting, validation, conceptualization.

FUNDING

This work is supported by National Key Research and Development Program of China under Grant no. 2018YFB1305700 and Scientific and Technological Program of Quanzhou City under Grant No. 2019CT009.

REFERENCES

1. Internation Telecomunications Union. ICT facts and figures 2017. *Itu* (2017) 1–8.
2. Riurean S, Antipova T, Rocha Á, Leba M, and Ionica A. VLC, OCC, IR and LiFi Reliable Optical Wireless Technologies to be Embedded in Medical Facilities and Medical Devices. *J Med Syst* (2019) 43:308. doi:10.1007/s10916-019-1434-y
3. Dat PT, Bekkali A, Kazaura K, Wakamori K, and Matsumoto M. A universal platform for ubiquitous wireless communications using radio over FSO system. *J Lightwave Technol* (2010) 28:2258–67. doi:10.1109/jlt.2010.2049641
4. Bohata J, Komanec M, Spáčil J, Ghassemlooy Z, Zvánovec S, and Slavík R. 24-26 GHz radio-over-fiber and free-space optics for fifth-generation systems. *Opt Lett* (2018) 43:1035–8. doi:10.1364/ol.43.001035
5. Khalighi MA, and Uysal M. Survey on free space optical communication: A communication theory perspective. *IEEE Commun Surv Tutorials* (2014) 16: 2231–58. doi:10.1109/comst.2014.2329501
6. Chaudhary S, and Amphawan A. The role and challenges of free-space optical systems. *J Opt Commun* (2014) 35:327–34. doi:10.1515/joc-2014-0004
7. Chaudhary S, and Amphawan A. High-speed millimeter communication through radio-over-free-space-optics network by mode-division multiplexing. *Opt Eng* (2017) 56:116112. doi:10.1117/1.oe.56.11.116112
8. Singh M, and Malhotra J. Performance comparison of high-speed long-reach mode division multiplexing-based radio over free space optics transmission system using different modulation formats under the effect of atmospheric turbulence. *Opt Eng* (2019) 58:046112. doi:10.1117/1.oe.58.4.046112
9. Dev K, Nebuloni R, Capsoni C, Fiser O, and Brazda V. Estimation of optical attenuation in reduced visibility conditions in different environments across free space optics link. *IET Microwaves, Antennas & Propagation* (2017) 11: 1708–13. doi:10.1049/iet-map.2016.0872
10. Xu H, Liu L, and Shi Y. Polarization-insensitive four-channel coarse wavelength-division (de)multiplexer based on Mach-Zehnder interferometers with bent directional couplers and polarization rotators. *Opt Lett* (2018) 43:1483–6. doi:10.1364/ol.43.001483
12. Pan Y, Yan L, Yi A, Chen Z, Jiang L, Pan W, et al. Transmission of three-polarization-multiplexed 25-Gb/s DPSK signals over 300-km fiber link. *Opt Lett* (2016) 41:1620–3. doi:10.1364/ol.41.001620
13. Geng Z, Corcoran B, Zhu C, and Lowery AJ. Time-lenses for time-division multiplexing of optical OFDM channels. *Opt Express* (2015) 23:29788–801. doi:10.1364/oe.23.029788
14. Mendoza-Yero O, Mínguez-Vega G, Martínez-León L, Carbonell-Leal M, Fernández-Alonso M, Doñate-Buendía C, et al. Diffraction-based phase calibration of spatial light modulators with binary phase Fresnel lenses. *J Display Technol* (2016) 12:1027–32. doi:10.1109/jdt.2016.2580902
15. Wang X, Ge D, Ding W, Wang Y, Gao S, Zhang X, et al. Hollow-core conjoined-tube fiber for penalty-free data transmission under offset launch conditions. *Opt Lett* (2019) 44:2145–8. doi:10.1364/ol.44.002145
16. Sheffi N, and Sadot D. Energy-efficient VCSEL array using power and offset allocation of spatial multiplexing in graded-index multimode fiber. *J Lightwave Technol* (2017) 35:2098–108. doi:10.1109/jlt.2017.2656238
17. Chaudhary S, and Amphawan A. Selective excitation of LG 00, LG 01, and LG 02 modes by a solid core PCF based mode selector in MDM-Ro-FSO transmission systems. *Laser Phys* (2018) 28:075106. doi:10.1088/1555-6611/aabd15

18. Ren Y, Wang Z, Liao P, Li L, Xie G, Huang H, et al. Experimental characterization of a 400 Gbit/s orbital angular momentum multiplexed free-space optical link over 120 m. *Opt Lett* (2016) 41:622–5. doi:10.1364/ol.41.000622
19. Grover A, Sheetal A, and Dhasarathan V. Performance analysis of mode division multiplexing based free space optics system incorporating on–off keying and polarization shift keying under dynamic environmental conditions. *Wireless Networks* (2020) 1–11.
20. Chaudhary S, Tang X, and Wei X. Comparison of Laguerre-Gaussian and Donut modes for MDM-WDM in OFDM-Ro-FSO transmission system. *AEU - Int J Elect Commun* (2018) 93:208–14. doi:10.1016/j.aeue.2018.06.024
21. Upadhyay KK, Shukla NK, and Chaudhary S. A high speed 100 Gbps MDM-SAC-OCDMA multimode transmission system for short haul communication. *Optik* (2020) 202:163665. doi:10.1016/j.ijleo.2019.163665
22. Minz M, Mishra D, Sonkar RK, and Khan MM. Grating-assisted MDM-PDM hybrid (de) multiplexer for optical interconnect applications. In: *Nanophotonics and Micro/Nano Optics V*. China: SPIE/COS Photonics Asia (2019). p. 111930C.
23. Ghatak A, and Thyagarajan K, *An introduction to fiber optics*. United Kingdom: Cambridge university press (1998). doi:10.1017/cbo9781139174770
24. Design O. *Optiwave Corporation 7 Capella Court Ottawa*. Ontario: Canada.
25. Bloom S, Korevaar E, Schuster J, and Willebrand H. Understanding the performance of free-space optics [Invited]. *J Opt Netw* (2003) 2:178–200. doi:10.1364/jon.2.000178
26. Andrews LC, and Phillips RL. *Laser beam propagation through random media*, vol. 152. WA: SPIE press Bellingham (2005).
27. Kim II, McArthur B, and Korevaar EJ. Comparison of laser beam propagation at 785 nm and 1550 nm in fog and haze for optical wireless communications. In: *Optical Wireless Communications*, III. China: SPIE (2001). p. 26–37.
28. Majumdar AK. Free-space laser communication performance in the atmospheric channel. *J Optic Comm Rep* (2005) 2:345–96. doi:10.1007/s10297-005-0054-0

Conflict of Interest: The authors declare that the research was conducted in the absence of any commercial or financial relationships that could be construed as a potential conflict of interest.